

1995 NASA/ASEE SUMMER FACULTY FELLOWSHIP PROGRAMM

JOHN F. KENNEDY SPACE CENTER  
UNIVERSITY OF CENTRAL FLORIDA

511-37

7751

P. 33

DESIGN OPTIMIZATION OF A BRUSH TURBINE  
WITH A CLEANER/WATER BASED SOLUTION

Dr. Rhyn H. Kim  
Professor

Department of Mechanical Engineering and Engineering Science  
University of North Carolina at Charlotte  
Charlotte, North Carolina

KSC Colleague - Rudy Werlink  
Fluids

Contract Number NASA-NGT-60002  
Supplement 19

July 21, 1995

#### ACKNOWLEDGEMENT

I would like to acknowledge that I have been privileged to participate in the FACULTY SUMMER PROGRAM in KENNEDY SPACE CENTER sponsored by NASA in 1994 and 1995. I appreciate the assistance offered by the Coordinator staff, Drs. Anderson and Hosler particularly help in the area of the paper work given by Ms. Kari Stiles of University of Central Florida.

I have enjoyed working with Mr. Rudy Werlink, KSC colleague who has helped me whenever I needed in the real engineering and office oriented problems. I thank Dr. Gary Lin, former chief of the branch for his consistent interest on the subject I have spent time for two years.

The last but not least, I acknowledge my office mate, Prof. Pao-lin Wang for his continuous encouragement, and a moral support given to me during the tenure of the assignment in KSC.

## ABSTRACT

Recently, a turbine-brush was analyzed based on the energy conservation and the force momentum equation with an empirical relationship of the drag coefficient. An equation was derived to predict the rotational speed of the turbine-brush in terms of the blade angle, number of blades, rest of geometries of the turbine-brush and the incoming velocity. Using the observed flow conditions, drag coefficients were determined. Based on the experimental values as boundary conditions, the turbine-brush flows were numerically simulated to understand first the nature of the flows, and to extend the observed drag coefficient to a flow without holding the turbine-brush.

### SUMMARY

One of methods of cleaning fouling in tubes will be a turbine-brush unit to replace R113 as a cleaner after 1995. The turbine-brush consists of a turbine and a brush with a connector between the two. The turbine-brush was created in KSC,NASA and demonstrated its rotational motion while it was held at a position.

Objective of the program is to optimize the geometry of the turbine-brush in terms of the blade angle, the number of blades, and arrangements of the connector and brush, flow rates, rotational speeds, diameters of tubing and performance of cleaning before a final product is designed and manufactured.

A prediction of a rotational speed was made without considering the blade angle in the beginning stage of the project and later the blade angle was taken into account. In the analysis of rotation speeds, empirical relations were used for drag forces. The drag forces were determined in a situation where the turbine-brush was held in a position. One suspects whether the drag force measured in this way would be the same as the unit moves. Because of this reason, a numerical simulation was thought of as a method of understanding the nature of the flow in a turbine-brush flow and of determining a way to use the simulation technique to a freely moving turbine-brush unit i tubes.

NEKTON was available for analyzing a simulation model. A simplified model, and an improved model for the blade section were made and these models were being tested. It seems that a superposition method of two solutions, one out of a rotating model and the second one of that model without rotation in a turbulent flow should be sought for a final simulation of the turbine-brush flows.

TABLE OF CONTENTS

Section	Title
	Cover/Title Page
	Acknowledgement
	Abstract
	Summary
	List of Figures
	Nomenclatures
I	INTRODUCTION
II	APPROACH TO A SIMULATION
2.1	Geometric Model
2.2	Construction of NEKTON Network
III	GOVERNING EQUATIONS
3.1	Continuity
3.2	Equation of Motion
3.3	Model for Turbulent Flows
IV	BOUNDARY CONDITIONS
4.1	Pressure Boundary
4.2	Boundary Conditions for Velocity
V	MATERIAL PROPERTIES
VI	SOLUTION METHOD
6.1	Current Status of Computations
VII	MODIFYING EQUATION FOR PREDICTING ROTATION SPEED
7.1	An Equation for An Angular Velocity
VIII	Experiments with a Closed Loop Apparatus
IX	CONCLUDING REMARKS
X	REFERENCES
XI	APPENDIX

## LIST OF FIGURES

- Figure 1. Sketch of the turbine-brush
- Figure 2. Discretization of flow domain
- Figure 3. Current model for the turbine
- Figure 4. Discretization of entrance section
- Figure 5. Discretization of blade section
- Figure 6. Discretization of connectors
- Figure 7. Discretization of brush
- Figure 8. Discretization of leaving section
- Figure 9. Refined blade model
- Figure 10. Pressure on an inner element expressed  
in a function of a constant
- Figure 11. Velocity boundary conditions next to a solid  
surface
- Figure 12a. Front view of the first segment of the blade
- Figure 12b. Front view of the 2nd segment of the blade
- Figure 12c. Front view of the 3rd segment of the blade
- Figure 12d. Front view of the 7th segment of the blade
- Figure 12e. Front view of the 8th segment of the blade
- Figure 12f. Front view of the 9th segment of the blade
- Figure 13. Orientation of blade placement with respect to  
the rotation axis
- Figure 14. A closed loop experimental set-up

## NOMENCLATURE

A	Area of a flow cross-section, m <sup>2</sup>
a	Constant used in the boundary conditions
b	Constant used in the boundary conditions
C <sub>1f</sub>	Constant used in the boundary conditions
C <sub>2t</sub>	Constant used in the turbulence model
C <sub>3t</sub>	Constant used in the turbulence model
C <sub>μ</sub>	Constant used in the turbulence model
c	Constant used in the boundary conditions
d	Diameter of the tube, m
E	Available energy for rotation Joule/m <sup>3</sup>
F(x,t)	Function used in the boundary condition
F <sub>i</sub>	Body force in the i-the direction
G <sub>b</sub>	Function used in the turbulence due to buoyancy
G <sub>k</sub>	Function used in the turbulence due to dissipation kinetic energy
g <sub>i</sub>	Gravitational acceleration, m <sup>2</sup> /s
J <sup>total</sup>	Sum of the moment of inertia of rotating elements
mdot	Mass rate, Kg/s
P	Static pressure, pa
Q	Volume rate along the blades, m <sup>3</sup> /s
S <sub>m</sub>	Mass source of dispersed states
t	time, s
(Δt) <sup>2</sup>	Convergence criterion
u <sub>1</sub>	Tangential velocity component in the y-direction
u <sub>i</sub>	Velocity component in the i-the direction
u <sub>n</sub>	Velocity component to normal to the surface
u <sub>x</sub>	Velocity component in the x-direction
u <sub>y</sub>	Velocity component in the y-direction
u <sub>z</sub>	Velocity component in the z-direction
u <sub>i</sub> u <sub>j</sub>	Reynolds stress
V	Velocity, m/s
W <sub>drag</sub>	Rate of work of drag
W <sub>kinetic</sub>	Rate of work due to rotation
x <sub>i</sub>	coordinates

## Greek Letters

β	Angle between the relative velocity and tangential velocity
δ <sub>ij</sub>	Kronecker delta
ε	Dissipation energy in turbulence
κ	Dissipation kinetic energy
μ	Molecular viscosity
μ <sub>t</sub>	Turbulent kinematic viscosity
v <sub>eddy</sub>	Turbulent kinematic viscosity
ρ	Density of the fluid
τ <sub>ij</sub>	Shear stress tensor
σ <sub>h</sub>	Constant defined in the turbulence model
σ <sub>ε</sub>	Constant defined in the turbulence model
ω	Angular velocity

## I. INTRODUCTION

CFC refrigerants/cleansers will not be allowed to use in cleaning fouling in tubes starting in 1996. A mechanical device was devised to clean inner surfaces of tubes in order to cope with the situation in which R113 is not available as a cleanser. An analytical expression of an angular velocity of the turbine-brush was developed in terms of geometries of the unit, the blade angle, number of blades, and the incoming velocity of the flow. The expression includes a drag coefficient which was derived from a series of experiments from an open loop and a closed loop experimental set-ups, respectively.

A numerical simulation was conducted first to understand the nature of the turbine-brush flows as the unit rotated while it was held at a position, and second to determine whether the numerical simulation may be extended to a case in which the turbine-brush moves forward while it rotates. For this purpose, a simplified model was developed and tested. An improved numerical model for the blade was also developed for further test.

At present, a numerical simulation with the simple model has not been completed. The test data from the closed loop set-up have not been analyzed, yet. The parts which are not completed will be further looked into on campus of UNC-Charlotte.

## II. APPROACH TO A SIMULATION

A numerical simulation was conducted for the turbine-brush flows by NEKTON of FLUENT Inc.

NEKTON is based on a finite element method incorporated with a spectral element technique originated by Patera(1984). This scheme employs a five point interpolating polynomial, known as the Legendre polynomial on a finite element network. As a result of the higher order power series, the software produces a fast converging numerical result with a relatively crude element network. However, this works for Stokes flows of a low Reynolds number up to 12,000 with a  $K-\epsilon$  turbulence model(Fluent, Inc., 1994).

The results of the numerical simulation will be compared with the results of experiments in terms of pressure and velocity distributions. The results of the lower Reynolds number flows may not represent the real flow conditions at all because of simplifying assumptions to build a model for simulation. In the beginning of simulation procedures, a relatively easy construction of the grid network and low rotational speed of the turbine brush lead to a use of NEKTON. Simplifying assumptions will be explained in later sections.



The procedure and result of the simulation analysis give a first hand insight in generating the elements and flow patterns. Application of this sort, a brush in the region of wake generated by a turbine, did not exist in a real world. The turbine brush was invented and its patent application was submitted in November 1993.

## 2.1 Geometric Model

A simplified geometric model is explained as follows. The simplified model is a first step for an eventual success of the simulation. Rather than the transient rotation of the turbine, steady angular velocity or a tangential velocity is assumed for the turbine-brush. Four blades are placed normal to the direction of the flow  $90^\circ$  apart in the outer race of a bearing. The bearing is located at the center of a blade housing. A wire is attached to the center of the bearing in such a way that the turbine-brush can rotate being held in a position. The liquid turbine and the rotating part of the bearing are connected to the brush by a two bar linkage, consequently make the brush rotating. The brush cleans fouling from the surface of the tube.

The first section of the simplified geometric model is the entering section of a fluid. The distance of this section is  $1d$ ,  $d$  being the diameter of the tube, since an incoming velocity of the flow is uniform. The second section consists of the entire structure of the turbine including the ring, blades, and bearing. The ring, blades and bearing are simplified to be a circular plate with four radial bars on each side. The turbine ring holds an O-ring so that the fluid may not pass the blade section in the direction of tube axis but moves in radial direction through the ring section of the turbine. The turbine runs without the O-ring. The third section is the connecting linkage. The fourth section is the brush section including the brush hub and a cut-off brush in four places separated equal distance along the circumference. It is assumed that fluid does not pass at all through the brush. The last two sections are the flow leaving sections which will be of a distance of  $(5 \text{ to } 8)d$ . A sketch of the turbine-brush is shown in Figure 1. A discretization of the flow domain is illustrated in Figure 2.

## 2.2 Construction of a NEKTON Network

A main idea of finite element construction in a three dimensional flow domain for NEKTON is to make a two-dimensional element on a plane and extend it along the third axis. Finite elements should have four vertices on the plane, and the four vertices should be specified in the counter-clockwise direction. Since a five point interpolating scheme is used between two connecting points, a crude initial network is affordable. The element network can use global refinement techniques, such as 'zipper', 'picture frame', 'corner' and so forth. Thereby, an easier construction of elements is possible. The number of elements of an

initial model is a little over one hundred and are shown in Figures 3-8. Figure 9 shows a sketch of a cross-section of the blade cut on the mid section of the flow. It also shows the steps of constructing the improved model for the blade by taking a thinner segment along the direction of the flow with the help of the global refinement of NEKTON procedures. Pressure and velocity boundary conditions on different elements are illustrated in Figures 10 and 11.

Starting with Figures 12a through 12f, the continuously increasing blade sections are shown for the improved model.

### III. GOVERNING EQUATIONS

A system of equations consists of continuity, and momentum equations. Since the temperature variations are not considered in this investigation, the energy equation is not needed.

#### 3.1 Continuity

Mass conservation law, known as the continuity equation is:

$$\frac{\partial \rho}{\partial t} + \frac{\partial}{\partial x_i} (\rho u_i) = S_m$$

where  $\rho$  is the density,  $t$  is the time,  $u_i$  are the velocity components, and  $x_i$  are the coordinate variables. Equation (1) is the general form of the mass conservation equation and valid for incompressible as well as compressible flows. The source  $S_m$  is the mass added to the continuous phase from the dispersed second phase, i.e., due to vaporization of liquid droplets.

#### 3.2 Equation of Motion

Conservation of momentum in the  $i$ -th direction in an inertial reference frame is described by (Schlichting, 1960):

$$\frac{\partial}{\partial t} (\rho u_i) + \frac{\partial}{\partial x_j} (\rho u_i u_j) = -\frac{\partial p}{\partial x_i} + \rho g_i + F_i$$

where  $p$  is the static pressure,  $\tau_{ij}$  is the stress tensor (described below), and  $g_i$  and  $F_i$  are gravitational acceleration and external

body forces in the  $i$  direction, respectively.

The stress  $\tau_{ij}$  is given by:

$$9 \tau_{ij} = \left[ \mu \left( \frac{\partial u_i}{\partial x_j} + \frac{\partial u_j}{\partial x_i} \right) \right] - \frac{2}{3} \mu \frac{\partial u_k}{\partial x_k} \delta_{ij}$$

where  $\mu$  is the molecular viscosity and the second term on the right hand side is summed over all three component directions. In the computation, the term  $(2/3)\mu(\partial u_k/\partial x_k)$  is ignored under the assumption that the divergence of velocity has a negligible effect on the stresses.

### 3.3 Model for Turbulent Flows

Modeling of turbulent flows requires appropriate modeling procedures to describe the effects of turbulent fluctuations of velocity and scalar quantities on the basic conservation equations presented in the previous section. The  $\tau$ - $\epsilon$  turbulence model is a basic model from which a turbulence is described. This model is an eddy-viscosity model in which the Reynolds stresses are assumed to be proportional to the mean velocity gradients, with the constant of proportionality being the turbulent eddy viscosity,  $\mu_t$ . This assumption, known as the Boussinesq hypothesis, provides the following expression for the Reynolds stresses (Fluent, Inc., 1994):

$$\overline{\rho u_i u_j} = \rho \frac{2}{3} \kappa \delta_{ij} - \mu_t \left( \frac{\partial u_i}{\partial x_j} + \frac{\partial u_j}{\partial x_i} \right) + \frac{2}{3} \mu_t \frac{\partial u_i}{\partial x_i} \delta_{ij}$$

Here  $\kappa$  is the turbulent kinetic energy:

$$\kappa = \frac{1}{2} \sum_i \overline{u_i^2}$$

The term  $(2/3)\mu_t(\partial u_i/\partial x_i)$  is ignored under the assumption that the divergence of velocity has a negligible effect on the turbulent stress tensor. The equation for the Reynolds stresses is analogous to that describing the shear stresses that arise in laminar flow

with the turbulent viscosity  $\mu_t$  playing the same role as the molecular viscosity  $\mu$ . Therefore the form of the turbulent momentum equations remain identical to the form of the laminar momentum equation except that  $\mu$  is replaced by an effective viscosity,  $\mu_{\text{eff}} = \mu + \mu_t$ . The turbulent viscosity  $\mu_t$  is obtained by assuming that it is proportional to the product of a turbulent velocity scale and length scale.

In the  $\kappa$ - $\epsilon$  model, these velocity and length scales are obtained from two parameters:  $\kappa$ , the turbulent kinetic energy and  $\epsilon$ , the dissipation rate of  $\kappa$ . The velocity scale is taken to be  $\kappa=5$  and the length scale is taken to be  $\kappa^{3/2}/\epsilon$ . Hence,  $\mu_t$  is given by:

$$\mu_t = \rho C_\mu \frac{\kappa^2}{\epsilon}$$

where  $C_\mu$  is an empirically derived constant of proportionality (set to a default value of 0.09). The values of  $\kappa$  and  $\epsilon$  are obtained by solution of conservation equations (Fluent, Inc., 1994):

$$\frac{\partial}{\partial t} (\rho \kappa) + \frac{\partial}{\partial x_j} (\rho u_j \kappa) = \frac{\partial}{\partial x_j} \left( \frac{\mu_t}{\sigma_\kappa} \frac{\partial \kappa}{\partial x_j} \right) + G_\kappa + G_b - \rho \epsilon$$

$$\frac{\partial}{\partial t} (\rho \epsilon) + \frac{\partial}{\partial x_j} (\rho u_j \epsilon) = \frac{\partial}{\partial x_j} \left( \frac{\mu_t}{\sigma_\epsilon} \frac{\partial \epsilon}{\partial x_j} \right) +$$

$$C_{1\epsilon} \frac{\epsilon}{\kappa} (G_\kappa + (1 - C_{3\epsilon}) G_b) - C_{2\epsilon} \rho \frac{\epsilon^2}{\kappa}$$

where  $C_{1\epsilon}$  and  $C_{2\epsilon}$  are empirical constants,  $\sigma_\kappa$  and  $\sigma_\epsilon$  are "Prandtl" numbers governing the turbulent diffusion of  $\kappa$  and  $\epsilon$ ,  $G_\kappa$  is the rate of production of turbulent kinetic energy:

$$G_k = \mu_t \left( \frac{\partial u_j}{\partial x_i} + \frac{\partial u_i}{\partial x_j} \right) \frac{\partial u_i}{\partial x_j}$$

and  $G_b$  is generation of turbulence due to buoyancy:

$$G_b = -g_i \frac{\mu_t}{\rho \sigma_h} \frac{\partial \rho}{\partial x_i}$$

The above equations are applied to minimizing energy principle, in return, one obtains a series of finite element based equations. These equations are solved under physical boundary conditions. Actually, these boundary conditions are derived from experiments.

#### IV. BOUNDARY CONDITIONS

Two types of boundary conditions for elements exist in the flow domain in consideration. The first is on the boundary surface of each element, and the second is on the element itself. There are also conditions of the inlet and exit of the flow. Variables involved with the boundary conditions are the pressure and velocity. The first condition we consider is an incoming velocity. Unless otherwise specified, the incoming velocity is fully developed, meaning that either a uniform speed or a profile of the velocity of the flow is known. A simulation analysis yields the velocity at the exit of the flow field. Variations of velocity at the exit are usually shown in the region of 7 to 9d downstream of the inlet. These are identified VELOCITY and OUTFLOW.

##### 4.1 Pressure Boundary

The pressure is reduced as the fluid flows due to friction and changes in cross-sections of the flow passages. In general, this is expressed as:

$$\partial p / \partial x + F(x, t) = 0$$

where  $p$  is the static pressure,  $x$ , the coordinate in the flow

direction,  $t$ , the time and  $F$  is a function in  $x$  and  $t$ .

#### 4.2 Boundary Conditions for Velocity

The fluid is in contact with a stationary surface (inner surface of conduits) and with a moving surface (blades, ring structure, connector, and brush). In continuum condition, the velocity does not exist at the stationary surface:

$$u_x = 0, u_y = 0, \text{ and } u_z = 0$$

On the other hand, at the moving boundary, the fluid layer next to the surface, moves with the same speed as the surface and expressions of velocity components are given by:

$$u_n = 0, u_1 = 0, u_2 = r\omega = \omega(y^2 + z^2)^{0.5}$$

where  $u_n$  is the component of the velocity normal the surface,  $u_1$  is the first tangential ( $y$ -axis) component, and  $u_2$  is the second tangential component ( $z$ -axis) of the velocity.

For each element of the fluid in the field, the above boundary conditions entered. A partial list of elements and their boundary conditions are shown in Appendix starting with the element 1 through the element 4 and element 328. In the list, initial conditions of the velocity is also provided.

Specifically, the current project uses the following for the above expression.

Incoming velocity,  $u_x = f(x)$  or constant,  $u_y = 0$ , and

$$u_z = 0$$

Pressure,  $pa = a - bx$

Moving Layer,  $u_n = 0, u_1 = 0,$   
 $u_2 = c * (y^2 + z^2)^{0.5}$

where  $a$ ,  $b$ , and  $c$  are determined based on the specific runs of experiments. With an existing set of experimental data, the list shows those specific numbers. A sinusoidal equation is assigned for  $u_x$  to indicate that the at the end of the turbine-brush unit,  $u_x$  vanishes, implying that only the rotational speed influences the flow domain.

### 4.3 Body Force

The force holding the turbine-brush at a point is considered a body force opposite to the flow direction.

## V. MATERIAL PROPERTIES

The fluid in consideration is liquid water at room conditions. Therefore, variables in mind are the density and viscosity which are constant because the temperature variation is not considered.

## VI. SOLUTION METHOD

NEKTON provides a unsteady solution for three dimensional Navier-Stokes problems. The convective terms are treated explicitly by using a third order Adams-Bashforth multiple step scheme which is accurate to  $O(\Delta t^2)$ . The diffusion terms are treated implicitly by using a third order backward differentiation multistep scheme. For problems with time-dependent domains, the geometry is updated explicitly using a third order Adams-Bashforth multistep scheme.

Once an element network is constructed, an input file is submitted into the SOLVER of NEKTON. Based on error messages, the number of elements or of orders may be increased.

### 6.1 Current status of Computations

The first solution was tried with the number of elements of about 150. The NEKTON solver did not provide a converging solution. By using the global refinement techniques, the number of elements were increased to the neighborhood of 450. The upper limit of the three dimensional elements is 450. Thus, a consistent attention must be paid in a process of building elements.

There are two versions of the blade models. At present, the simplified version has been investigated. Because of a few reasons, a solution has not been produced yet. In order to determine whether the geometry of the model is possible at all, a flow of Reynolds number of 100 was tried. A result was produced. Therefore, the model used for simulation is possible.

Further trials will be made on campus of UNC-Charlotte. The trials will include the first and second models of the blade section as well as establishing the steady flows for the both models.

## VII. MODIFIED EQUATION FOR PREDICTING ROTATIONAL SPEEDS

Shepherd(1967) gives the required rotational energy in terms of an available energy for rotation as follows:

$$E = u_2(u_2 - Q/A_2 \cot\beta_2) - u_1(u_1 - Q/A_1 \cot\beta_1)$$

where  $Q$  is the volume rate flowing along the blades,  $A$ , the cross-section of the flow and the angle between the relative velocity of the flow rate and the tangential speed  $u$  is denoted as  $\beta$ (see Figure 13). Subscripts 1, and 2 refer to an entering and leaving sections, respectively. Applying the above equation to the turbine-brush with  $\beta_1 = \pi/2$ , one obtains the required energy for rotation as:

$$E = u_2(u_2 - Q/A_2 \cot\beta_2)$$

### 7.1. An Equation for the Angular Velocity

The existing turbine-brush has  $\beta_2 = \pi/4$ . Based on report(Kim,1994 and Kim and Werlink,1995), the conservation energy equation is given by:

$$W_{\text{drag}} + W_{\text{kinetic}} = \dot{m} \cdot [(P_{\text{exit}} - P_{\text{inlet}}) + (V_{\text{exit}}^2 - V_{\text{inlet}}^2)/2]$$

where  $W_{\text{drag}}$  is the rate of work due to the drag force and friction,  $W_{\text{kinetic}}$  is the minimum kinetic energy for the turbine-brush to rotate and is expressed as:

$$W_{\text{kinetic}} = J_{\text{total}} \cdot \omega^2 / 2$$

where  $J_{\text{total}}$  is the sum of moment of inertia of the entire rotating body and  $\dot{m}$  is given by:

$$\dot{m} = \rho V_{\text{inlet}} A_{\text{cube.cross}}$$

Therefore, a relation for the angular velocity  $\omega$  is obtained by optimizing the energy equation with respect to  $\omega$  under the constraints, the mass rate  $\geq 0$  and

$$E \geq W_{\text{drag}} + W_{\text{kinetic}}$$



### VIII. EXPERIMENTS WITH A CLOSED LOOP APPARATUS

A closed loop apparatus for the turbine-brush and its instrumentation were completed very late. Specially, a ultra-sonic volume rate readings device did not function properly, and a series of second testings were done again. Instrumentations were described elsewhere (Kim, 1994 and Kim and Werlink, 1995). The loop with the test section is shown in Figure 14. A quick inspection of the current data indicated that there are variations between the data of an open loop and closed loop systems. A careful investigation is necessary for the new set of data before any comparison is made between the current and old data sets.

### IX. CONCLUDING REMARKS

A numerical simulation of the turbine-brush flows was conducted with a simplified model and computations are on going. After a successful result comes from the simplified model, the improved blade model will be simulated. A series of new data sets were obtained from a closed loop fluid circuit. An analysis of the new data will be done.

Unfinished portions of the project will be reported as soon as possible.

### X. REFERENCES

- Fluent, Inc., 1993 NEKTON User' Guide
- Kim, R.H., 1994, Design optimization of a brush turbine with a cleaner/water based solution, 1994 NASA/ASEE summer faculty fellowship program, University of Central Florida, NASA-NGT-60002 Supplement: 17, pp. 313-338
- Kim, R.H. and Werlink, R.J., 1995, Analysis of a turbine-brush for cleaning fouling in tubes, Proceedings of Fluid Engineering, ASME, Fluid Machinery Forum, FED222, pp. 93-99
- Patera, A.T., 1984, Spectral Element Method for Fluid Dynamics: Laminar Flow in a Channel Expansion, J. of Computational Physics, Vol. 53(3), pp. 468-488
- Schlichting, H., 1960, Boundary Layer Theory, McGraw-Hill Book Co.
- Shepherd, D.G., 1967, Principles of turbomachinery, The Macmillan Co., pp. 65-74

X. APPENDIX

Abridged Input File

1000.00 DENSITY  
 0.108000E-02 VISCOS  
 0. BETAG  
 0. GTHETA  
 0. P5  
 0. P6

1.00000 RHOCF  
 1.00000 CONDUCT  
 0. QVOL

1.00000 FINTIME  
 NSTEPS  
 DT

0. IOCOMM  
 0. IOTIME  
 0. IOSTEP  
 0. MAXHIS  
 0. PATCHMESH

0.500000E-01 GRID  
 -1.00000 INTYPE  
 5.00000 NORDER  
 0. DIVERGENCE  
 0.100000E-03 HELMHOLTZ  
 0. NPSCAL

0.100000E-01 TOLREL  
 1.00000 TOLABS  
 0.250000 COURANT  
 2.00000 TORDER

0. TMESH  
 0. MAXCGHELM  
 0. POPRESSURE  
 0. GAS CONS R  
 0. Lo Ma GRAV

100.000 MXGEO  
 100.000 MAXNEW  
 0.100000E-03 TOLDIR  
 0.100000E-03 TOLNEW  
 0.100000E-01 TOLVNORMAL

0. SSFSLIMIT  
 0. P39

0. IFMAGNET  
 0. SIGMAMAG  
 0. SSFLENG  
 1.00000 VHScaleFac

0. POISSONRA  
 0. FSDFAC  
 0. IRSTART

0. CNFAC  
 0. PGEOM  
 0.140000 MIXLFAC  
 0. MAXCGFS

0. SETSIGMA  
 4.00000 REMESH  
 0. PRFSDATA  
 0. RAMPSTEPS  
 0. VRELAXFAC

4 Lines of passive scalar data follows2 CONDUCT; 2RHOCF  
 1.00000 1.00000 1.00000  
 1.00000 1.00000 1.00000  
 1.00000 1.00000 1.00000  
 1.00000 1.00000 1.00000

18 LOGICAL SWITCHES FOLLOW  
 T IFFLOW



```

E 327 1 326.000 3.00000 0. 0. 2to.
E 327 2 33.0000 4.00000 0. 0. 0.
E 327 3 320.000 1.00000 0. 0. 0.
E 327 4 54.0000 2.00000 0. 0. 0.
V 327 5 3.00000 1039.00 0. 0. 0.
ux=1.7*(1-sin(1.57*x/6.42))
uy=0
uz=0
V 327 6 3.00000 1042.00 0. 0. 0.
ux=1.7*(1-sin(1.57*x/6.42))
uy=0
uz=0
E 328 1 113.000 4.00000 0. 0. 0.
E 328 2 156.000 4.00000 0. 0. 0.
E 328 3 155.000 4.00000 0. 0. 0.
E 328 4 111.000 4.00000 0. 0. 0.
E 328 5 0. 0. 0. 0. 0.
E 328 6 90.0000 5.00000 0. 0. 0.
***** NO THERMAL BOUNDARY CONDITIONS *****
1 PRESOLVE/RESTART OPTIONS *****
PRESOLVE
7 INITIAL CONDITIONS *****
ux=1.7*(1-sin(3.14*x/6.42))
uy=0
uz=0
C Default
C Default
C Default
C Default

```

```

***** DRIVE FORCE DATA ***** BODY FORCE, FLOW, Q
4 Lines of Drive force data follow

```

```

ffx=51000
ffy=0
ffz=0

```

C \*\*\*\*\* Variable Property Data \*\*\*\*\* Overrides Parameter data.

```

1 Lines follow.
0 PACKETS OF DATA FOLLOW
***** HISTORY AND INTEGRAL DATA *****
6 POINTS. Hcode, I,J,H,IEL
UVWP H 2 3 4 303
UVWP H 5 5 3 110
UVWP H 5 5 2 110
UVWP H 3 3 1 162
UVWP H 2 3 1 162
UVWP H 5 3 5 24
***** OUTPUT FIELD SPECIFICATION *****
6 SPECIFICATIONS FOLLOW
COORDINATES
F VELOCITY
T PRESSURE
T TEMPERATURE
F TEMPERATURE GRADIENT
F PASSIVE SCALARS OUTPUTS
0 ***** OBJECT SPECIFICATION *****
0 Surface Objects
0 Volume Objects
0 Edge Objects
0 Point Objects
***** CURVED SIDE FORTRAN FUNCTIONS *****
0 Lines of Fortran

```

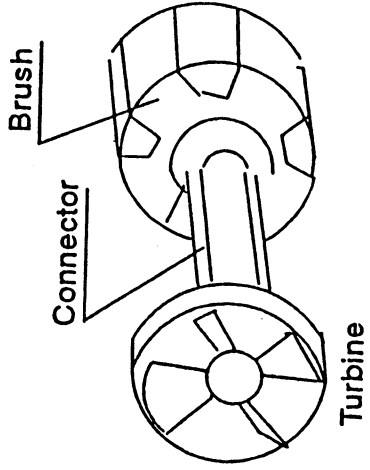
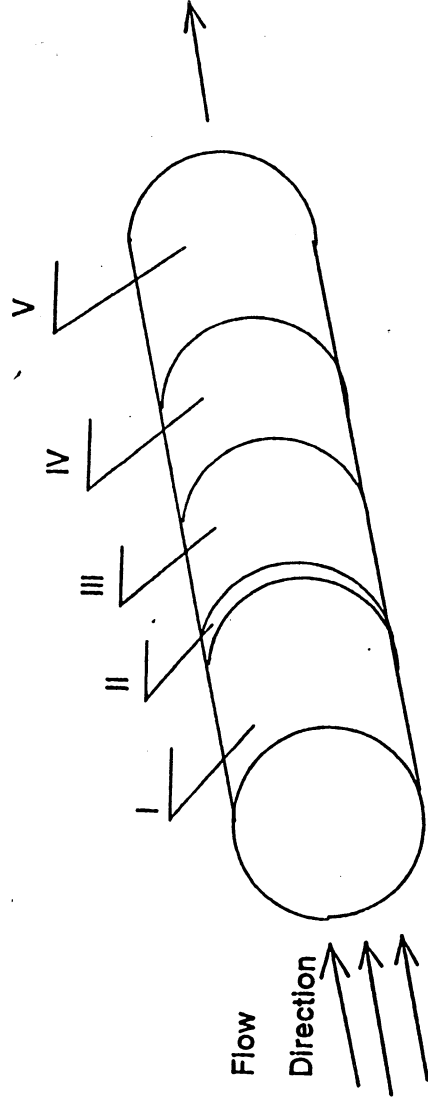


Figure 1. A Sketch of the turbine brush



I: Entrance Region, II: Turbine Section  
 III: Connector, IV: Brush Section  
 V: Exit Section of the Flow

Figure 2. Discretization of flow domain

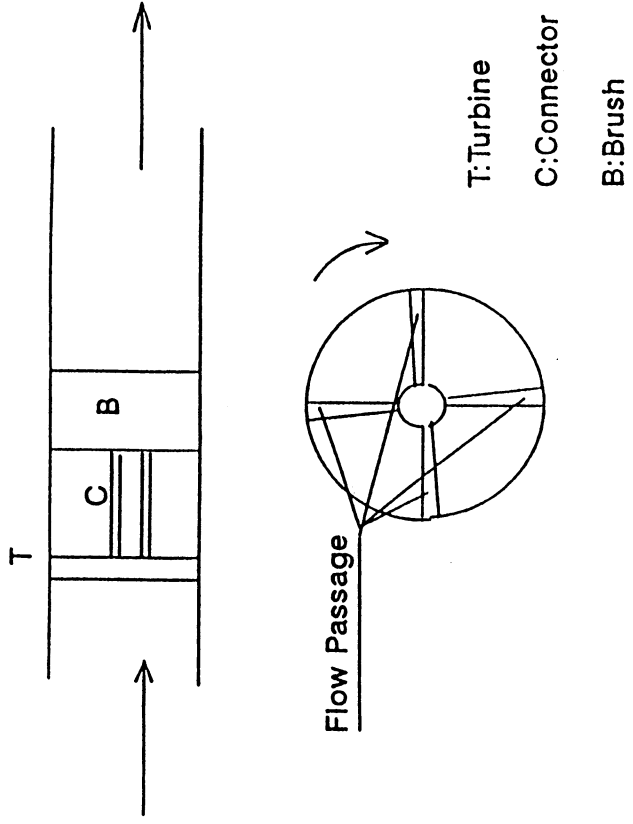


Figure 3. Current model for the turbine

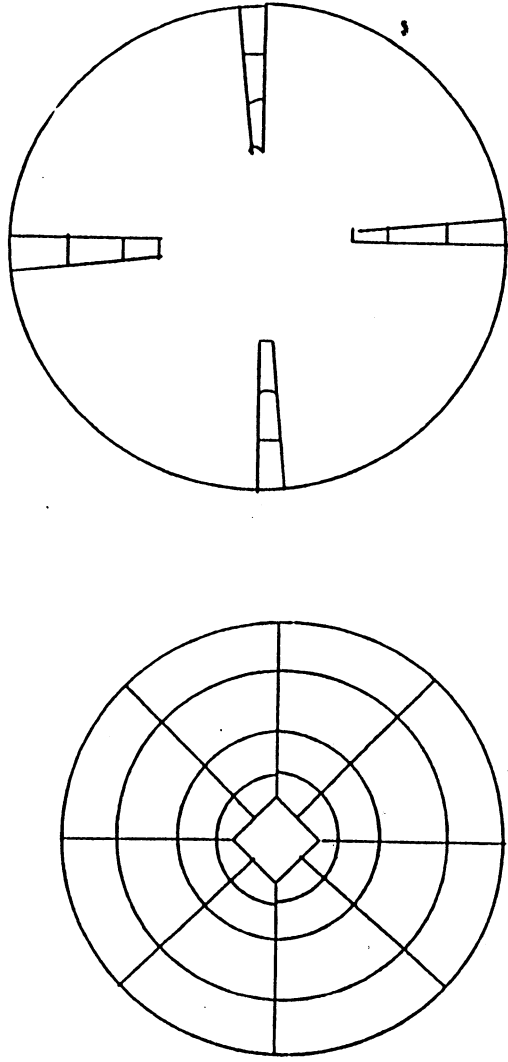


Figure 4. Discretization of Entrance Section

Figure 5. Discretization of Blade Section

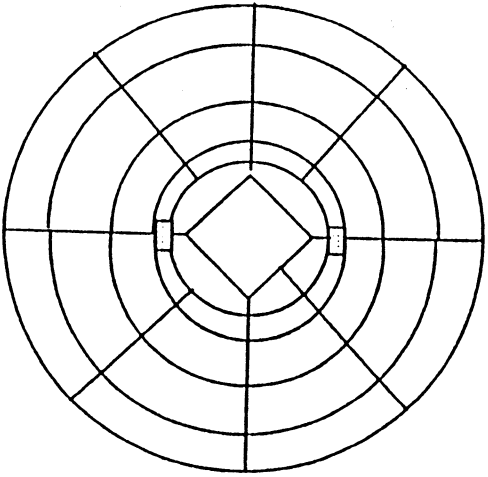


Figure 6. Discretization of Connectors

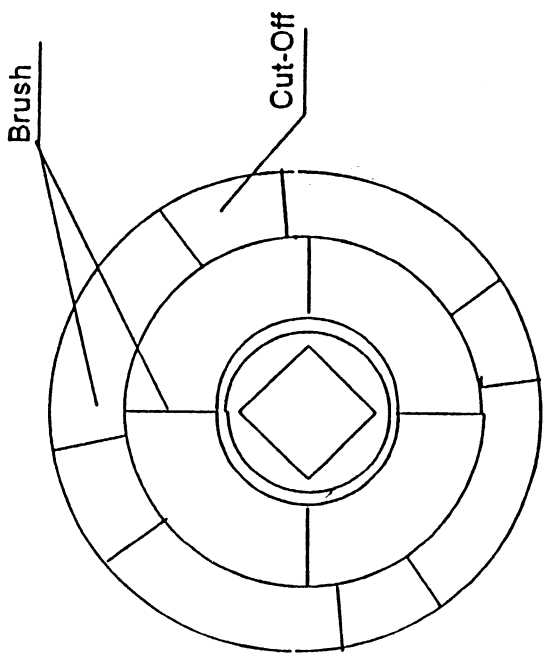


Figure 7. Discretization of Brush

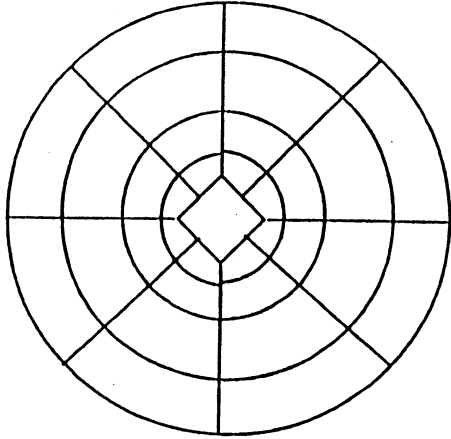


Figure 8. Discretization of Leaving Section



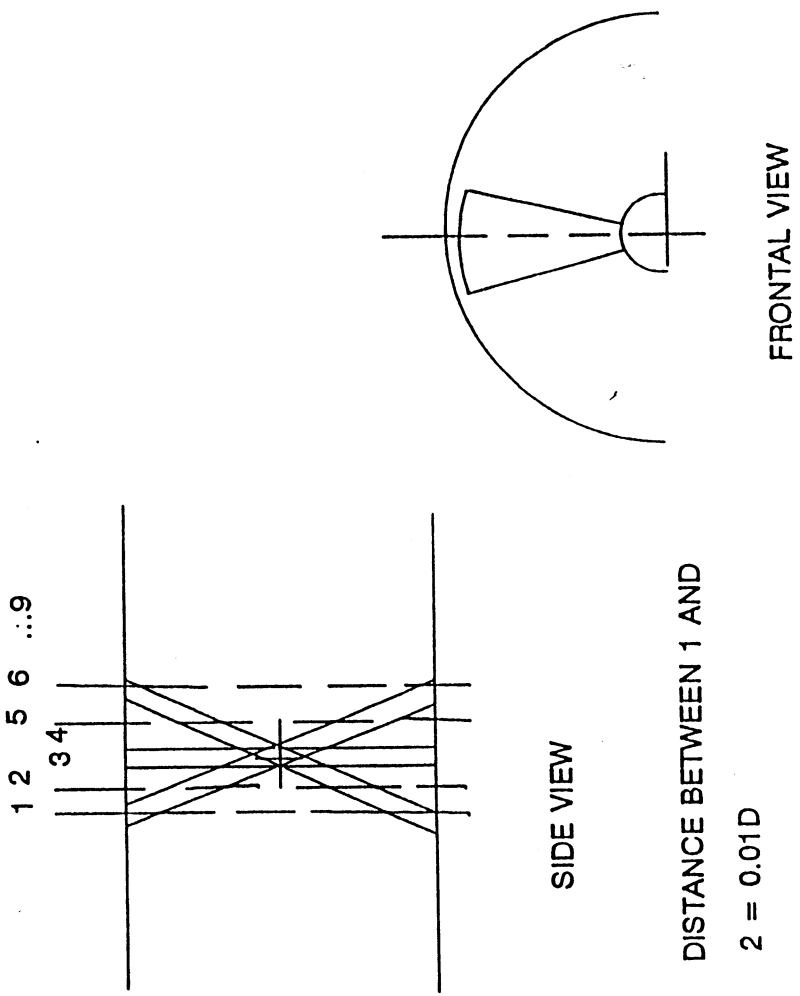


Figure 9.Refined Blade Model

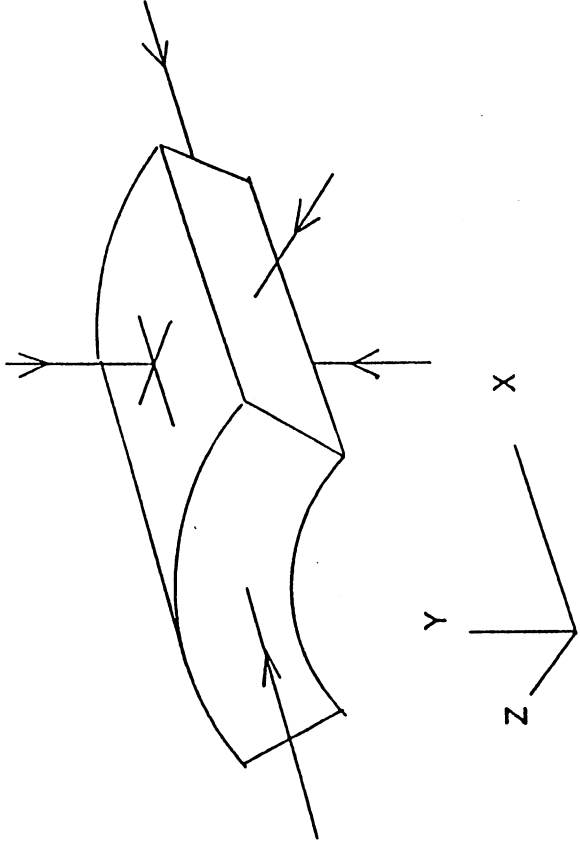


Figure 10.

PRESSURE ON AN INNER ELEMENT  
EXPRESSED IN A FUNCTION OF A CONSTANT

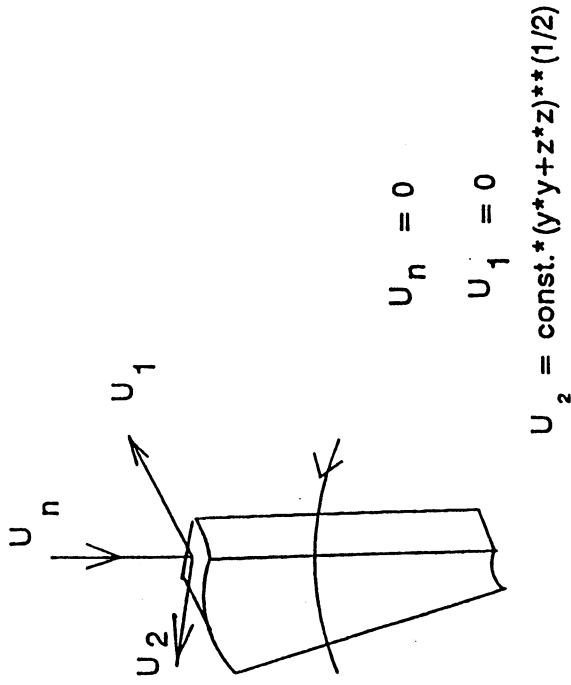


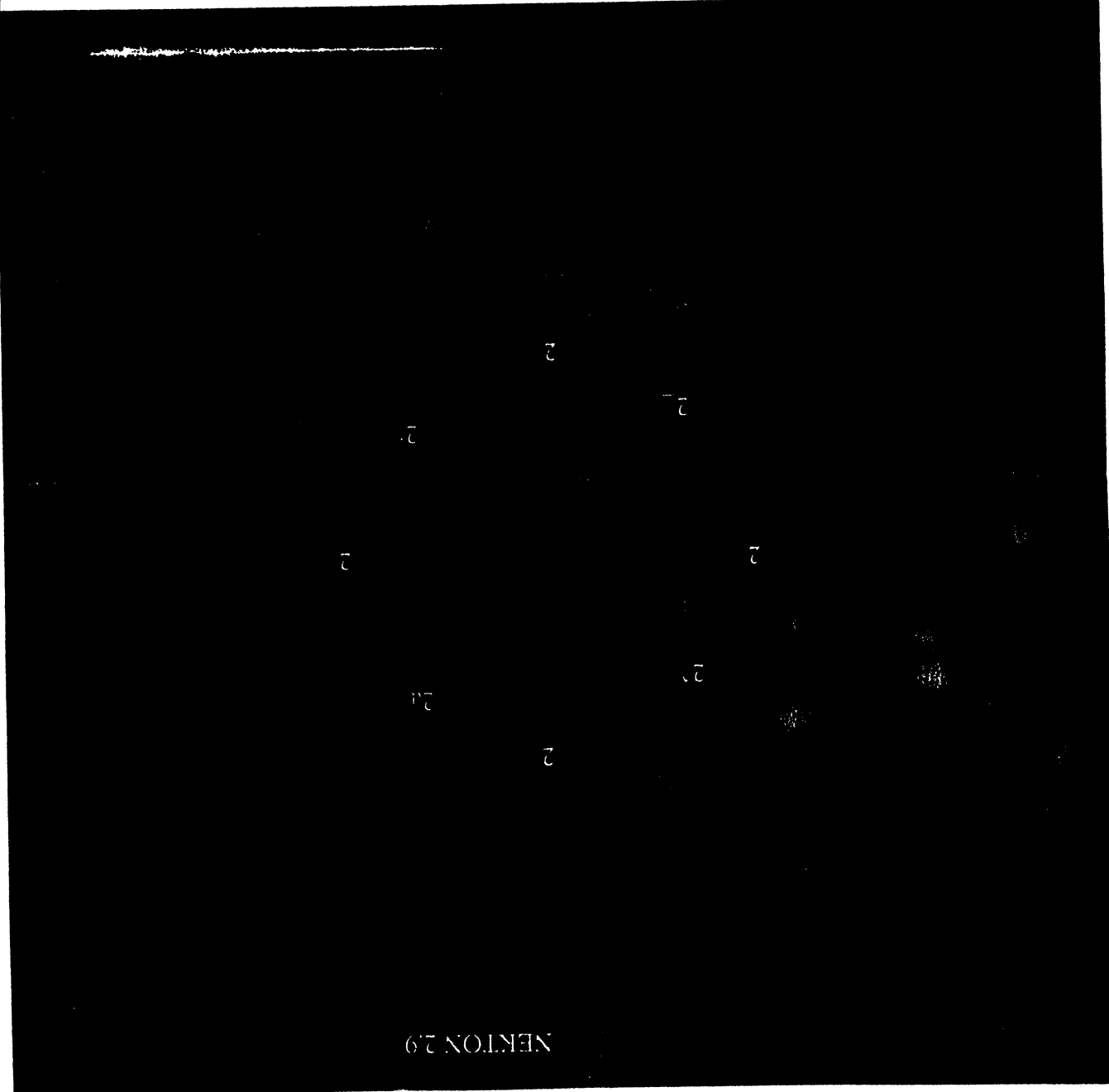
Figure 11.

Velocity Boundary Conditions  
Next to a Solid Surface

NEKTON  
V 2.9

Spectral Element Mesh from Prenek

Session Name: 070a

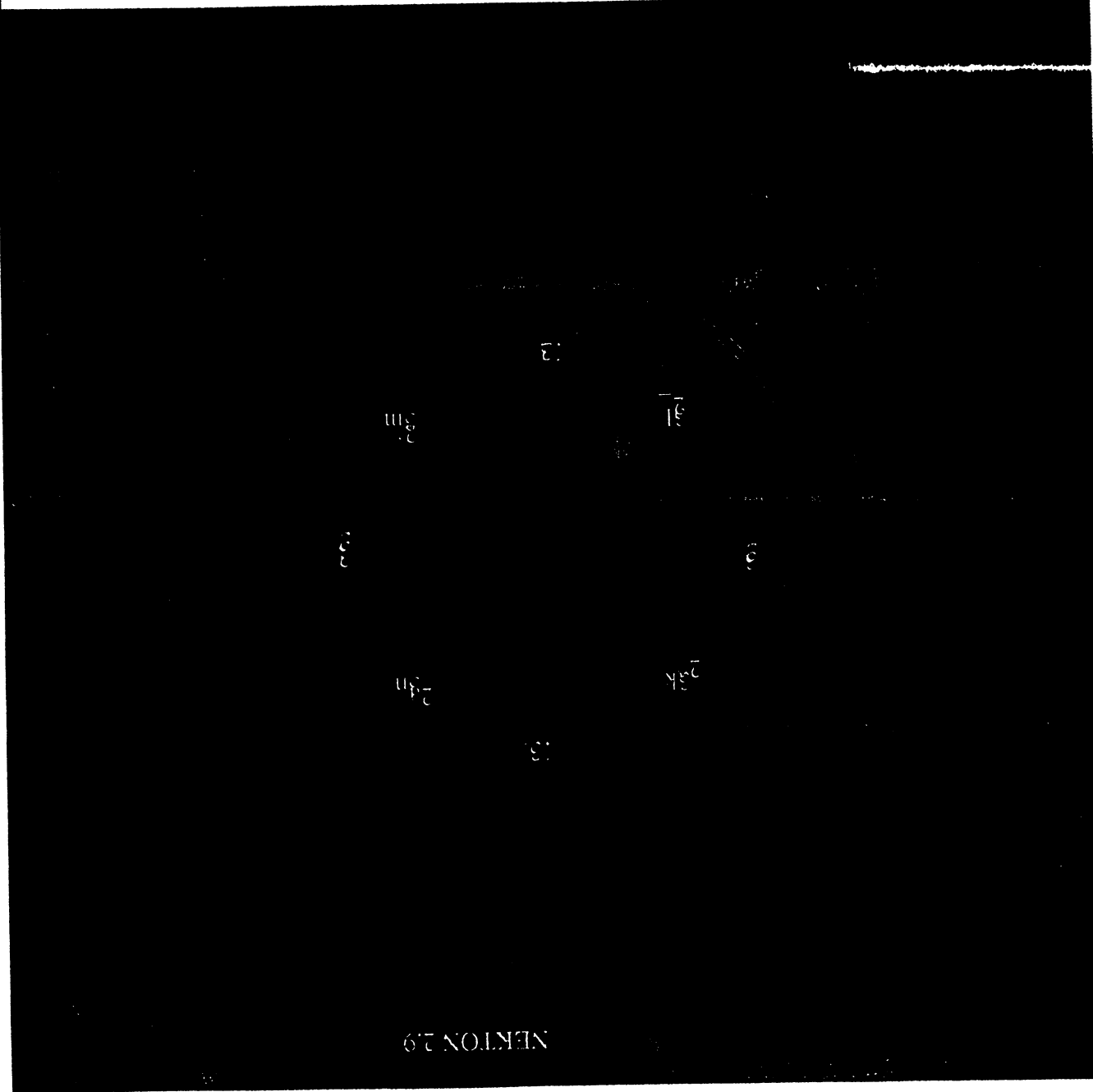


NEKTON 2.9

Figure 12a. Front view of the first segment of the blade

Spectral Element Mesh from Prenek

Session Name: 070b



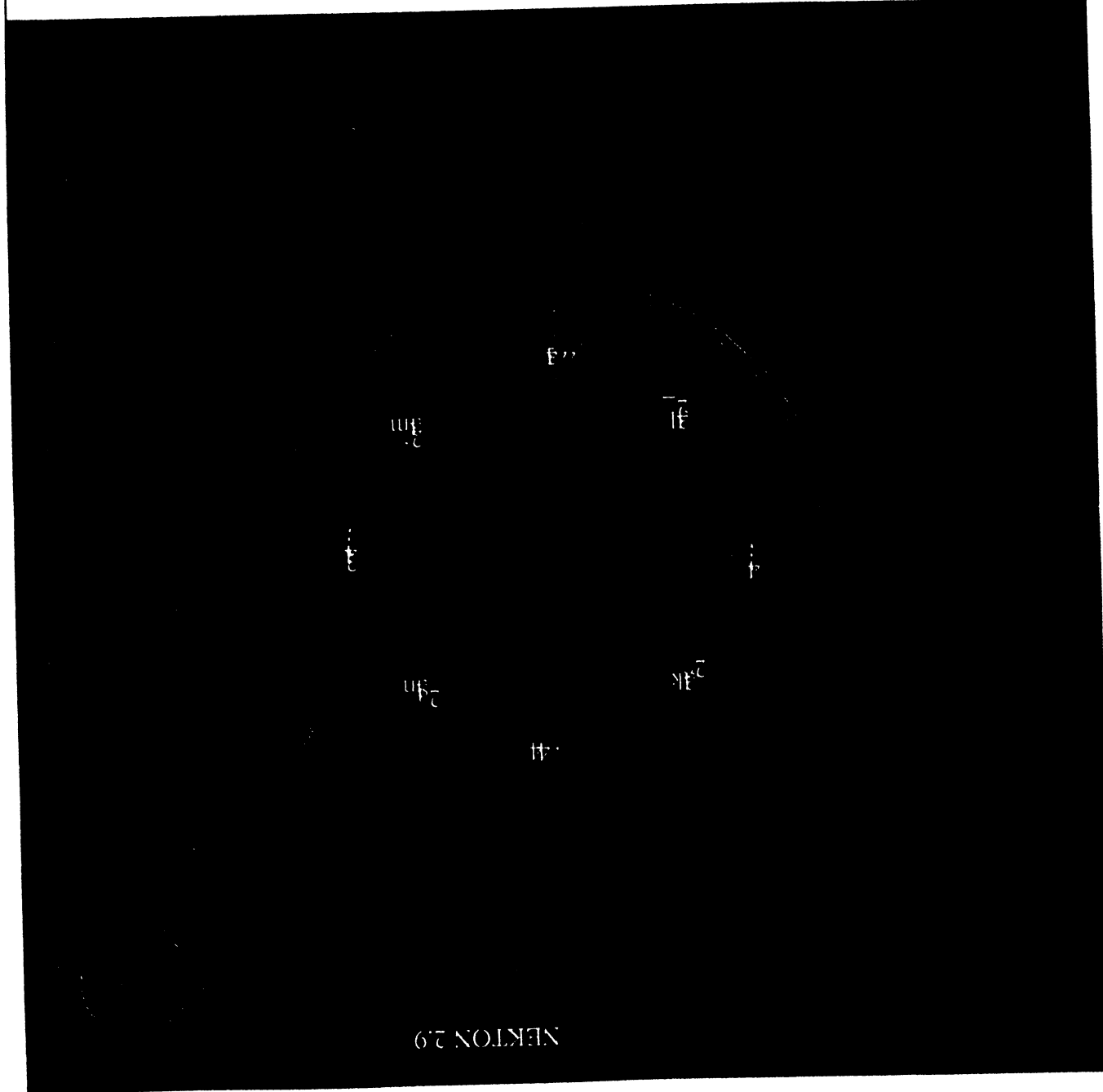
NEKTON 2.9

Figure 12b. Front view of the 2nd segment of the blade

NEKTON  
V 2.9

Session Name: 070a  
Spectral Element Mesh from Prenek

Figure 12c. Front view of the 3rd segment of the blade



NEKTON 2.9

NEKTON  
V 2.9

Session Name: 070d

Spectral Element Mesh from Prenek

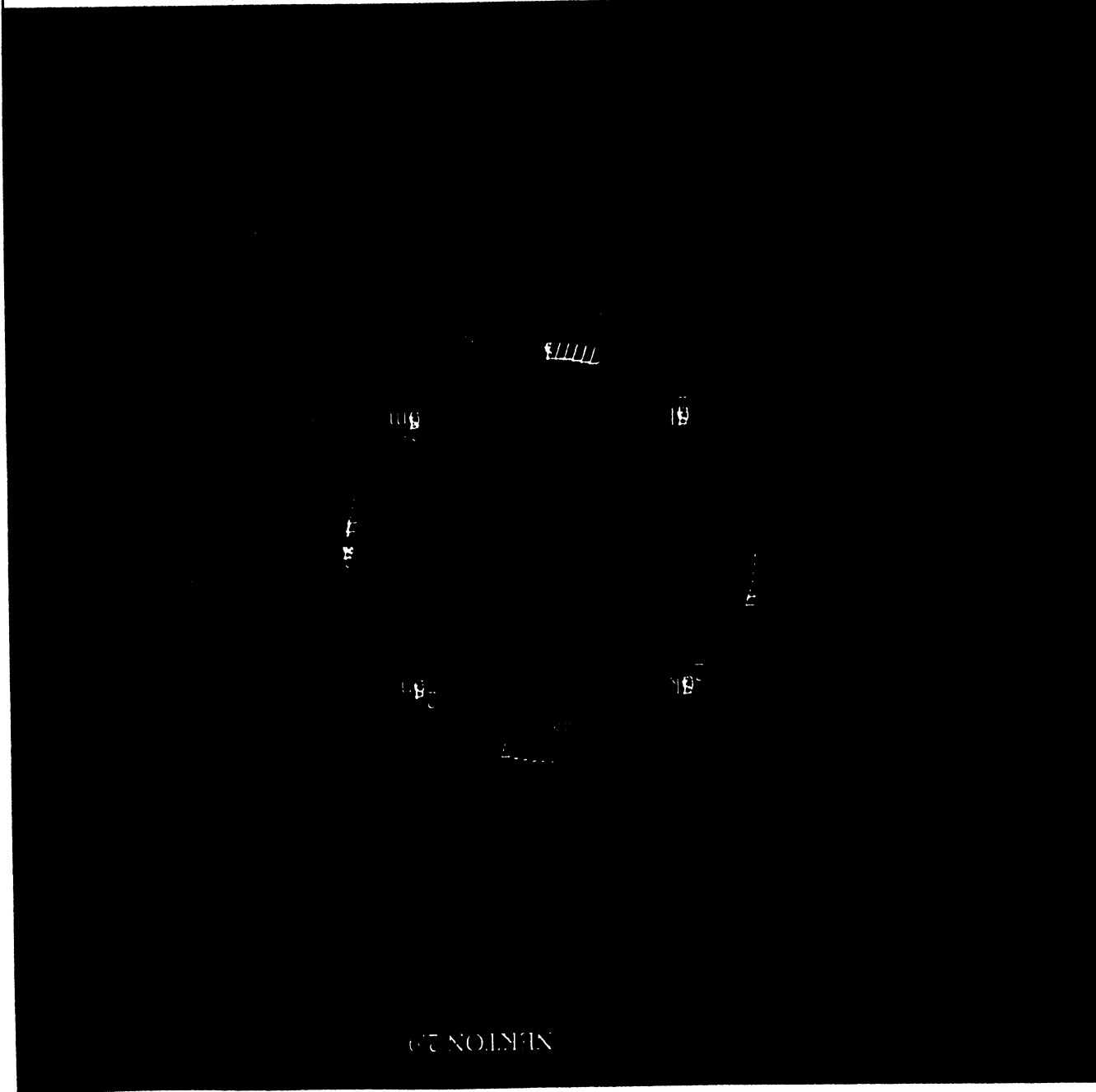


Figure 12d. Front view of the 7th segment of the blade

NEKTON  
V 2.9

Spectral Element Mesh from Pretek

Session Name: 070e

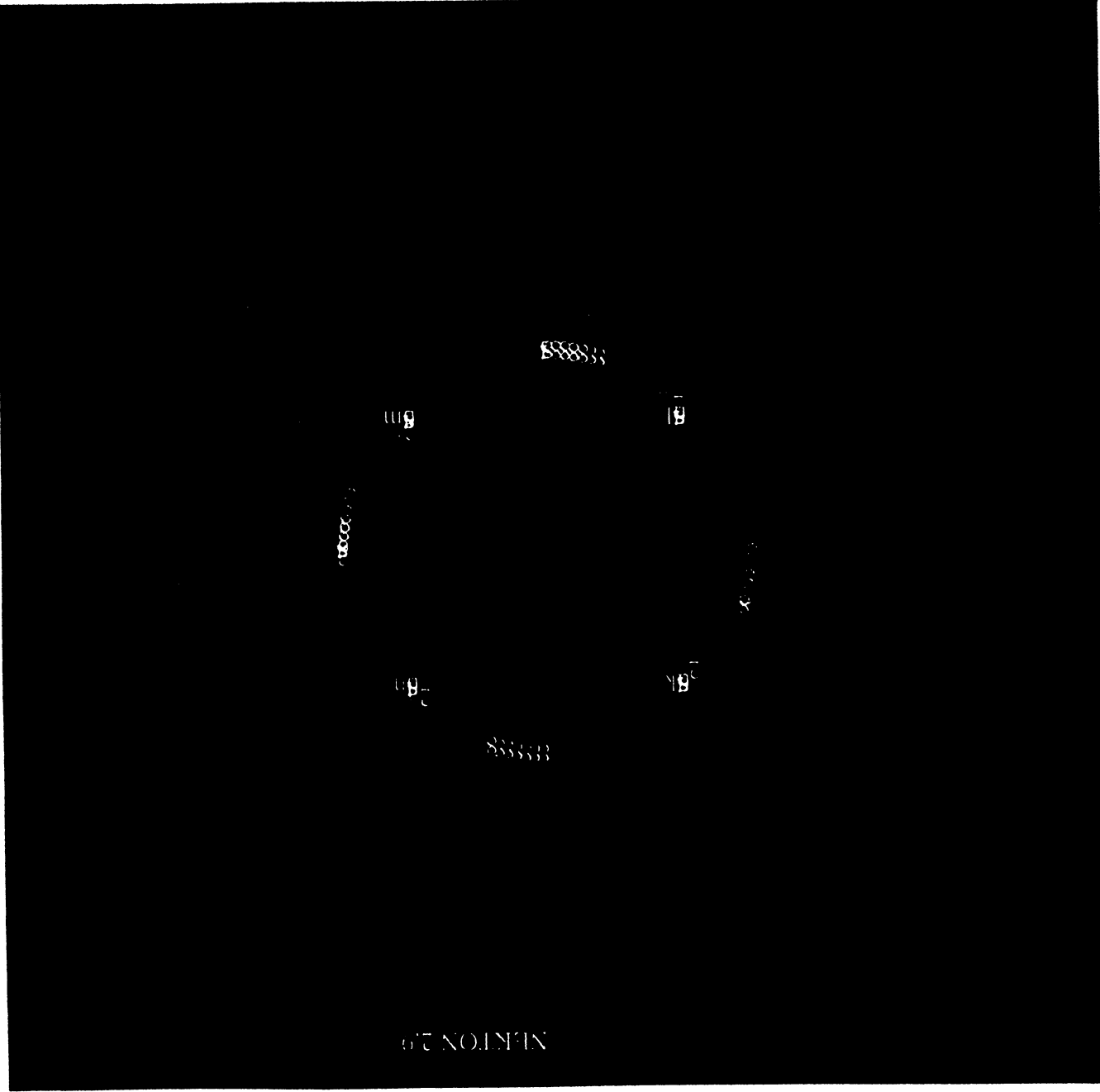
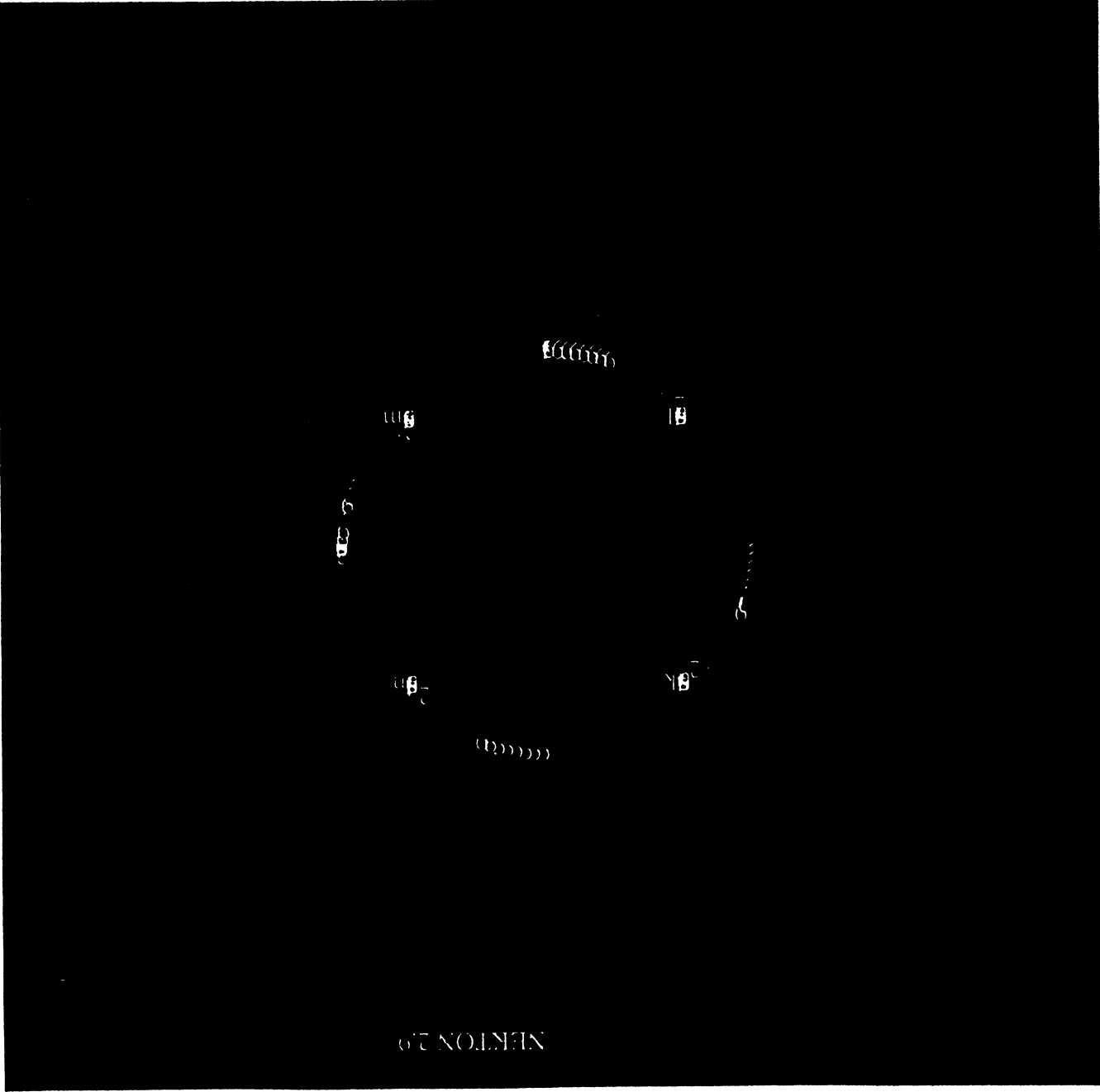


Figure 12e. Front View of the 8th segment of the blade

Session Name: J7195a

Spectral Element Mesh from Prenek

Figure 12f. Front view of the 9th segment of the blade





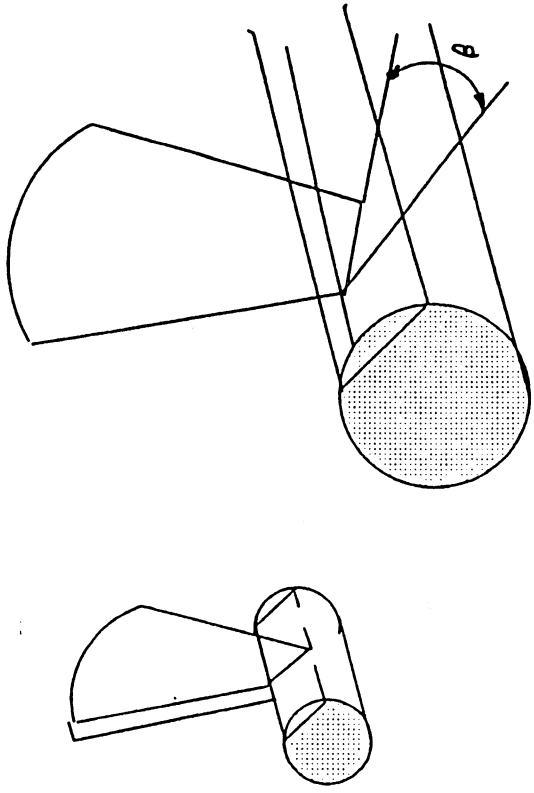


Figure 13. Orientation of Blade Placement with Respect to the Rotation Axis

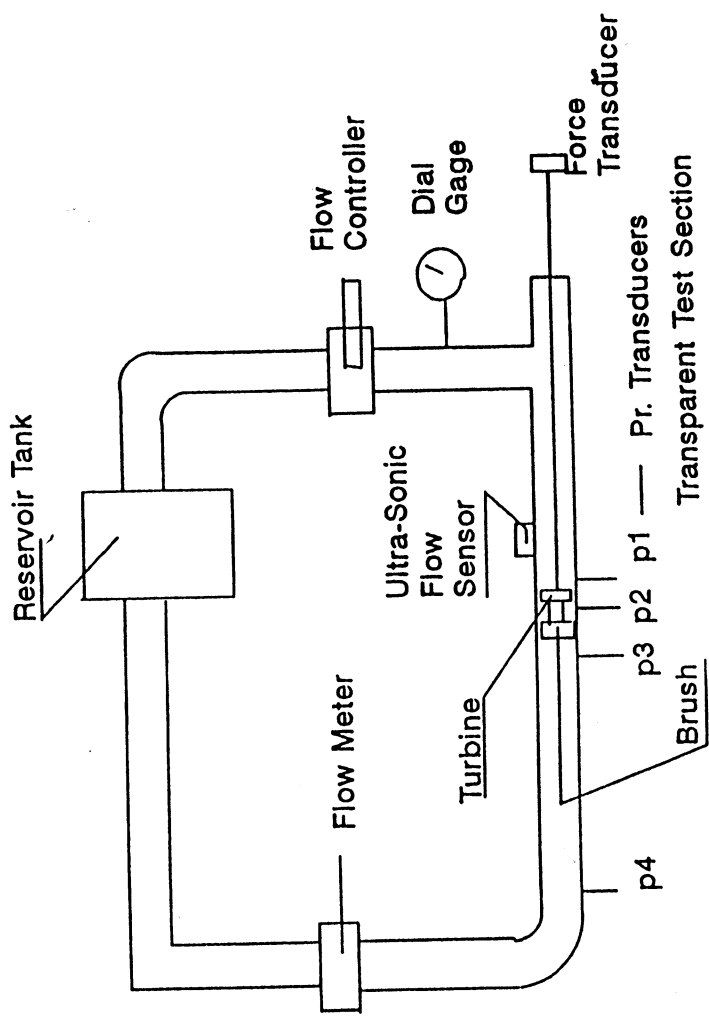


Figure 14. A Closed loop experimental set-up

